Original Research

Examining the technical feasibility of prostate cancer molecular imaging by transrectal photoacoustic tomography with transurethral illumination

Haonan Zhang[1,*], Shengsong Huang[2,*], Yingna Chen[1], Weiya Xie[1], Mengjiao Zhang[1], Jing Pan[1], Naoto Sato[3], Xueding Wang[1,4], Denglong Wu[2] and Qian Cheng[1]

[1]Institute of Acoustics, School of Physics Science and Engineering, Tongji University, Shanghai 200092, China; [2]Department of Urology, Tongji Hospital, Tongji University School of Medicine, Shanghai 200065, China; [3]Research and Development Department, CYBERDYNE, INC., Tsukuba, Ibaraki 3050818, Japan; [4]Department of Biomedical Engineering, University of Michigan, Ann Arbor, MI 48109, USA
Corresponding authors: Qian Cheng. Email: q.cheng@tongji.edu.cn; Denglong Wu. Email: wudenglong2009@tongji.edu.cn
*These authors contribute equally to this paper.

Impact statement

Differentiating cancerous tissues from healthy ones is critical in the diagnosis of prostate cancer (PCa). However, due to the low sensitivity of ultrasound (US) imaging to cancerous tissues, transrectal ultrasound (TRUS) guided biopsies, current standard procedure for diagnosing PCa, suffer from low core yield, leading to under-sampling and under-grading of clinically significant tumors. Via the experiment on the *ex vivo* human prostates, we evaluated the translational potential of photoacoustic imaging (PAI) based on a safe light emitting diodes (LED) source for detecting the molecular information in deep human prostate. We showed that transurethral light illumination in combination with transrectal US detection can facilitate PA molecular imaging over an entire human prostate in a non-invasive manner. The success of this study in the clinically relevant *ex vivo* human prostate model suggested a new strategy for PA and US combined imaging and detection of PCa.

Abstract

To pave the road toward clinical application of photoacoustic imaging in prostate cancer (PCa) diagnosis, we studied the technical feasibility and performance of transrectal photoacoustic (PA) imaging in mapping the indocyanine green (ICG) contrast agent, which is approved by FDA, in entire prostates by using light illumination via the urethral track. Experiments were conducted on a clinically relevant *ex vivo* model involving whole human prostates harvested from radical prostatectomy. The light source placed in the urethral track was an array of light emitting diodes (LEDs), illuminating the prostate with a delivered light power on the urethral wall within the safety limit. A dual-modality imaging system acquired PA and ultrasound (US) images simultaneously in the same way as in transrectal ultrasound (TRUS), with the US imaging presenting the tissue structure and PA imaging detecting the ICG solution. The imaging results demonstrated that tubes containing ICG solution at different concentrations can be detected at different positions in the prostate within a 2 cm range around from the urethral wall. Considering the sizes of regular human prostates, the proposed transurethral illumination in combination with transrectal US detection can facilitate PA molecular imaging over the entire prostate in a non-invasive manner, which makes it possible to further improve the PCa diagnosing efficiency with better molecular sensitivity and resulted better biopsy accuracy and much reduced pain for patients.

Keywords: Prostate cancer, TRUS, photoacoustic imaging, LED, transurethral illumination, ICG

***Experimental Biology and Medicine* 2020; 245: 313–320. DOI: 10.1177/1535370219884356**

Introduction

Transrectal ultrasound (TRUS) guided biopsy is currently the standard procedure for diagnosing prostate cancer (PCa). However, due to the low sensitivity of ultrasound (US) imaging to cancerous tissues, TRUS guided biopsies suffer from low core yield, leading to under-sampling and under-grading of clinically significant tumors. An advanced imaging technology which is capable of detecting prostate cancer *in vivo*, in real time, and can differentiate

aggressive tumors from non-aggressive ones will offer more accurate guidance to needle biopsy. Fluorescent imaging technology, with advantages including the high sensitivity in probing the functional and molecular information, has been explored for possible contributions to urologic surgeries.[1,2] The clinical application of fluorescence imaging in guiding prostate cancer needle biopsy, however, is impeded by its limited spatial resolution, especially the depth resolution, as well as the limited imaging depth.

The emerging photoacoustic (PA) imaging technology is capable of mapping the optical absorption contrast in deep biological tissue with excellent ultrasonic resolution. Combining the advantages of US imaging and fluorescence imaging, PA imaging offers a great potential to solve the long-standing challenges in prostate cancer diagnosis.[3] In previous studies, imaging prostate cancer by PA technologies has been proposed, and the feasibility of PA imaging in detecting subsurface lesions and vessels in prostates in a transrectal fashion has been explored by computational modeling and the experiments on animal models and human subjects.[4–7] Most of the experimental results suggest that prostate lesions within a distance of two centimeters from the rectal wall can be accessible by transrectal PA imaging. Although this imaging depth covers the majority of the peripheral zone of human prostate which is more prone to tumor development, other more distant zones in the prostate can be out of the imaging range. Recently, aiming at better coverage of human prostate, PA imaging with transurethral illumination as an alternative solution has been proposed.[8–10] The findings from computational simulations suggest that a combination of transurethral light illumination and transrectal ultrasonic detection can lead to an optimized configuration for prostate PA imaging.[8,9] The experiments following this imaging geometry have been conducted on canine prostates with implanted brachytherapy seeds to validate its feasibility.[10]

Besides detecting prostate tumors based on the endogenous contrast provided by hemoglobin, PA imaging of prostate cancer can also be powered by a variety of contrast agents with strong optical absorption such as those based on metallic nanoparticles (NPs) or containing organic dyes.[11–15] The contrast agents not only enhance the sensitivity of PA imaging in detecting tumors but also extend the scope of prostate cancer imaging from the tissue level to the molecular level by targeting cancer specific molecular biomarkers.[3] Via the experiments on the animal models, the specific uptakes of NPs by the prostate tumors and the contrast enhancement by the absorbing dyes in the NPs have been demonstrated.[12–15]

In this work, to pave the road toward clinical application, we studied the performance of PA imaging via transurethral illumination and transrectal ultrasonic detection in mapping the contrast agent labeled objects located over almost the entire human prostate. The objects were microtubes containing indocyanine green (ICG) dye which is FDA approved for clinical use. Unlike previous studies which mostly utilized class-IV lasers, an array of light emitting diodes (LEDs) was employed in this work as the light source for PA imaging. Using LED as the light source has many potential advantages, such as lower cost, smaller footprint of equipment, and better safety, which could contribute to the clinical translation of the PA imaging technology.[16]

Materials and methods

In this work, we studied the technical feasibility of PA imaging to cover the entire prostates by using LED light illumination via the urethral track. The experiments were conducted on whole human prostates *ex vivo*. Fresh human prostates from radical prostatectomy were provided by the urology clinic at the Tongji Hospital at Shanghai, China. All the prostates involved had sizes of 40–60 mL. All subjects gave their informed consent for inclusion before they participated in the study. The study was conducted in accordance with the Declaration of Helsinki, and the protocol was approved by the Ethics Committee of Tongji Hospital (2018–58).

The US and PA images of the prostate were acquired by an LED-based PA and US imaging system (AcousticX, CYBERDYNE, INC., Tsukuba, Japan) which has been introduced in a previous publication.[16] Unlike in the previous studies where two LED arrays were placed at the two sides of the linear probe for PA imaging in a reflection mode, a single LED array was involved in this study. The LED array has 144 elements, each with a size of 1.4 mm × 1.4 mm, as is shown in Figure 1(e). The 4 lines of 36 elements distribute on an area of 6.88 mm × 50.4 mm, providing 200 μJ pulse energy at 850 nm wavelength. Working with a pulse repetition rate of 4 KHz, extensive signal average can be conducted to enhance the signal-to-noise ratio (SNR). The LED-produced PA image and US image from a sample can be acquired simultaneously by this dual-modality system. A 128-element linear probe working at 9 MHz central frequency, the picture of which is given by Figure 1(d), was used to acquire the PA and US images.

To follow the situation of transurethral light illumination and transrectal ultrasonic detection, the LED array was placed in the urethra close to the center of the prostate, while the linear transducer probe was placed out of the prostate, as shown in Figure 1(a). A piece of porcine colon with a thickness of about 3 mm was placed between the surface of the probe and the prostate. Considering that the most common sizes of transurethral catheter are 10F (3.3 mm diameter) to 28F (9.3 mm diameter), a LED array with a size of 6.88 mm wide and 50.4 mm long has no problem to be inserted into the urethra. However, in its current design, the thickness of the LED array is large (30 mm) due to the housing of the serving electric circuit. To place the LED in the urethra, we made a cut in the prostate along the line marked in Figure 1(a). The light from the LED array illuminated on the urethral wall with a power density of 2.6 $kW \cdot m^{-2}$ which is below the safety limit of 5.98 $kW \cdot m^{-2}$ according to the international electrotechnical commission (IEC) 62471.[17]

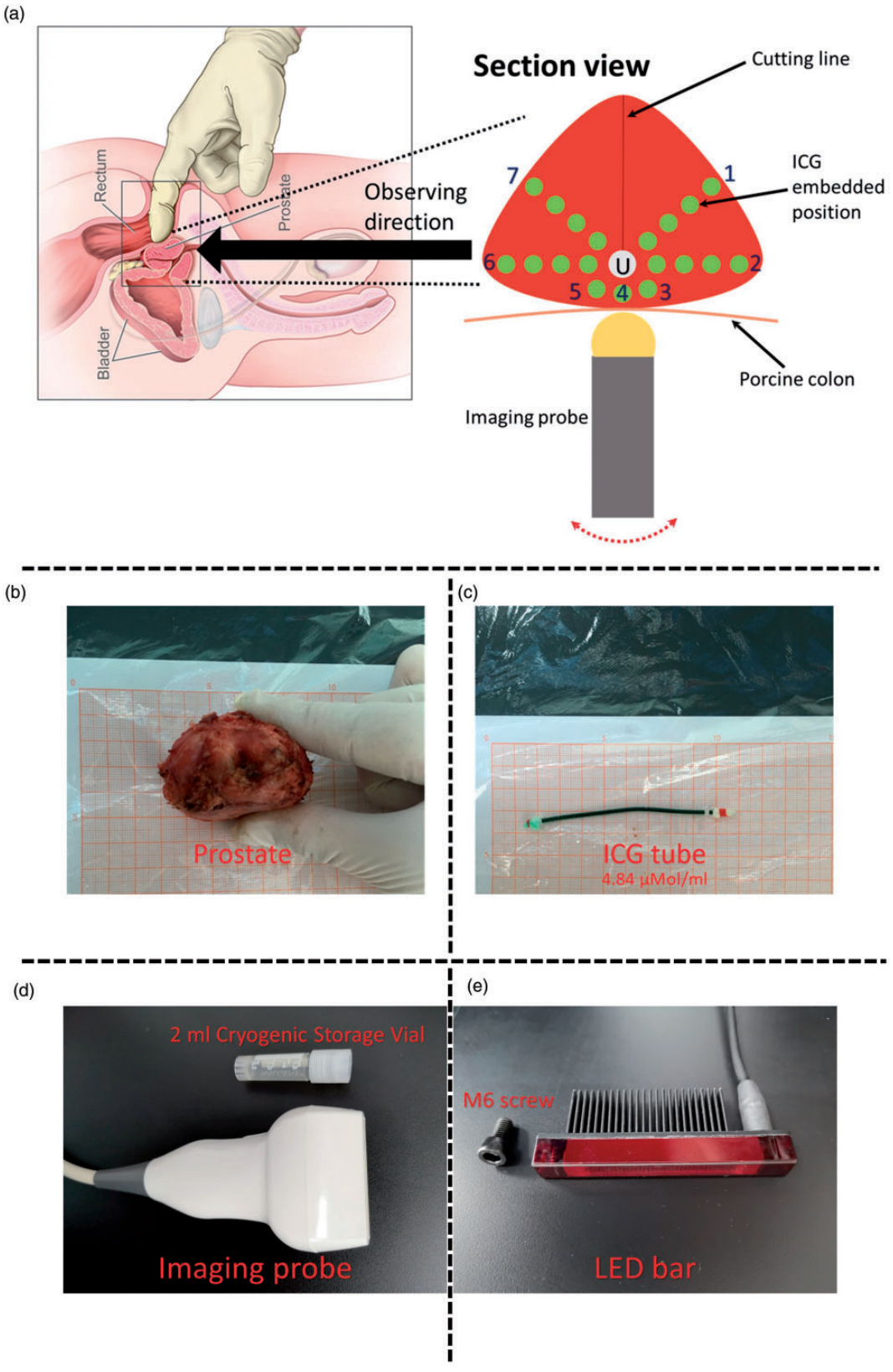

Figure 1. (a) Schematic of the experimental setup. 1–7 indicates the orientations of 45°, 90°, 135°, 180°, 225°, 270°, and 315°, respectively; U: urethra where the LED array placed. (b) Digital camera (DC) picture of a sample prostate. (c) DC picture of an ICG tube. (d) DC picture of the imaging probe. (e) DC picture of the LED bar. (A color version of this figure is available in the online journal.)

As shown in Figure 1(c), the imaging object was an optically transparent and soft plastic tube (inner diameter 1 mm; outer diameter 2 mm) filled with ICG solutions at different concentrations (4.84, 2.42, and 1.12 μMol/ml, respectively), mimicking the situation of a prostate tumor labeled with ICG contrast agent. The object was placed in the prostate at different positions around the urethra, along the seven orientations with angles of 45°, 90°, 135°, 180°, 225°, 270°, and 315°, respectively, from the vertical cutting line at the top of the prostate, as shown by the green dots in Figure 1(a). Along each orientation, the object was also placed at various distances from the urethra (e.g., 5, 10, 15, 20 mm). The number of positions (i.e. the optical depths) for each orientation is dependent on the thickness of the prostate tissue along that orientation. For example, since the prostate was thin along the 180° orientation, the object was only imaged at 5 mm optical depth; while along the orientations of 90° and 270° where the prostate was thick, the object was imaged at four different optical depths from 5 mm to 20 mm. The object was not placed at the 0° positions (i.e. the positions along the 12 o'clock orientation) because the image acquisition at these positions would be blocked by the LED light source placed in the urethra.

At each position, the ICG-containing tube was parallel to the urethra track, and was also parallel to the surface of the transducer probe. Before PA imaging of the object along each orientation, the surface of the LED array was rotated toward the object for more efficient light illuminate. In the future, the US scanning of the entire prostate can be combined with a rotating "searchlight" which could deliver light energy to certain orientations more efficiently than the sources giving isotopic illumination such as side-firing optical fiber bundles. To study the repeatability, PA and US imaging of the object at each position was repeated three times. In each time, the PA image was averaged over 1280 light pulses, leading to a PA imaging frame rate of 3.125 Hz. The contrast in imaging the ICG-containing object was quantified by the ratio between the maximal image intensity in the object area and the average image intensity in the background tissue. With the results from the three repeating imaging processes, the average and the standard deviation of the quantified contrast at each position were calculated.

Results

Figure 2 shows the example results of PA and US combined dual-modality imaging of the ICG-containing tube embedded at different positions covering all the regions inside a human prostate. In the experiment for Figure 2, the concentration of the ICG solution was kept at 4.84 μMol/ml. In each image, the PA image in pseudo color is superimposed on the gray-scale US image. The object can be recognized in every image, although the contrast is weaker when the optical depth is larger (e.g. the ones at 20 mm depth). Figure 3 shows the quantified contrast in PA imaging of the ICG-containing object in the prostate for each of the positions. Due to the light attenuation in the prostate tissue, the contrast as a function of the optical depth decreased quickly, following the pattern of exponential decay. However, even at the positions with an optical depth of 20 mm, the contrast between the object and the background tissue was still better than 2 dB.

The contrast in imaging the ICG-labelled object in prostate is not only dependent on the optical depth but also the ICG concentration in the object. In the next experiment the object was embedded at four different positions along the 90° orientation, with an optical depth changing from 5 mm to 20 mm. At each position, the concentration of the ICG in the tube was set at three different levels (4.84, 2.42, and 1.12 μMol/ml, respectively) for PA imaging. Figure 4 shows the example imaging results of the ICG-containing tube in a human prostate. Figure 5 shows the quantified contrast of the imaged object over the background prostate tissue as a function of the optical depth and the ICG concentration. As expected, the contrast decreases when the optical depth increases; also the contrast decreases when the ICG concentration decreases. Even at the smallest concentration of 1.12 μMol/ml, the ICG-containing tube can be imaged with a quantified contrast of 1.82 dB at an optical depth of 20 mm.

Discussion

The goal of this study on *ex vivo* human prostates from radical prostatectomy is to explore the technical feasibility of molecular imaging of prostate cancer by performing PA imaging via the transurethral illumination and transrectal detection. A pulsed LED array working at 850 nm wavelength was placed at the location of the urethra to illuminate the prostate. Performing with a light power density that is safe for human use, PA imaging of an ICG-labeled object was achieved with an optical depth up to 20 mm. Although the 20 mm depth is not the ultimate limit, considering that the light source in this imaging geometry is close to the center of the prostate, PA imaging with an optical depth of 20 mm is capable of covering almost all the positions in the entire whole human prostate.

The success of this study in the clinically relevant *ex vivo* human prostate model suggested that PA imaging powered by the optical contrast agents holds potential for more accurate guidance of needle biopsy. The PA imaging function can be readily integrated into the clinical standard TRUS without interference with the US imaging mode. Considering that the transurethral catheter is a commonly used procedure in urology clinic, a small size light source placed in the urethral track during TRUS is clinically feasible. A future PA and US dual-modality imaging following the similar protocol of TRUS would facilitate the imaging of both prostate morphology and the detection of contrast agent labeled tumors with excellent sensitivity and spatial resolution.

The designing concept of separating the light source and ultrasound probe involved in this study can be expanded to other applications. A miniaturized light source can be inserted into the open cavity of the target organ, e.g. a colon, while the ultrasound detection can be performed outside the human body. Such a design, by drastically

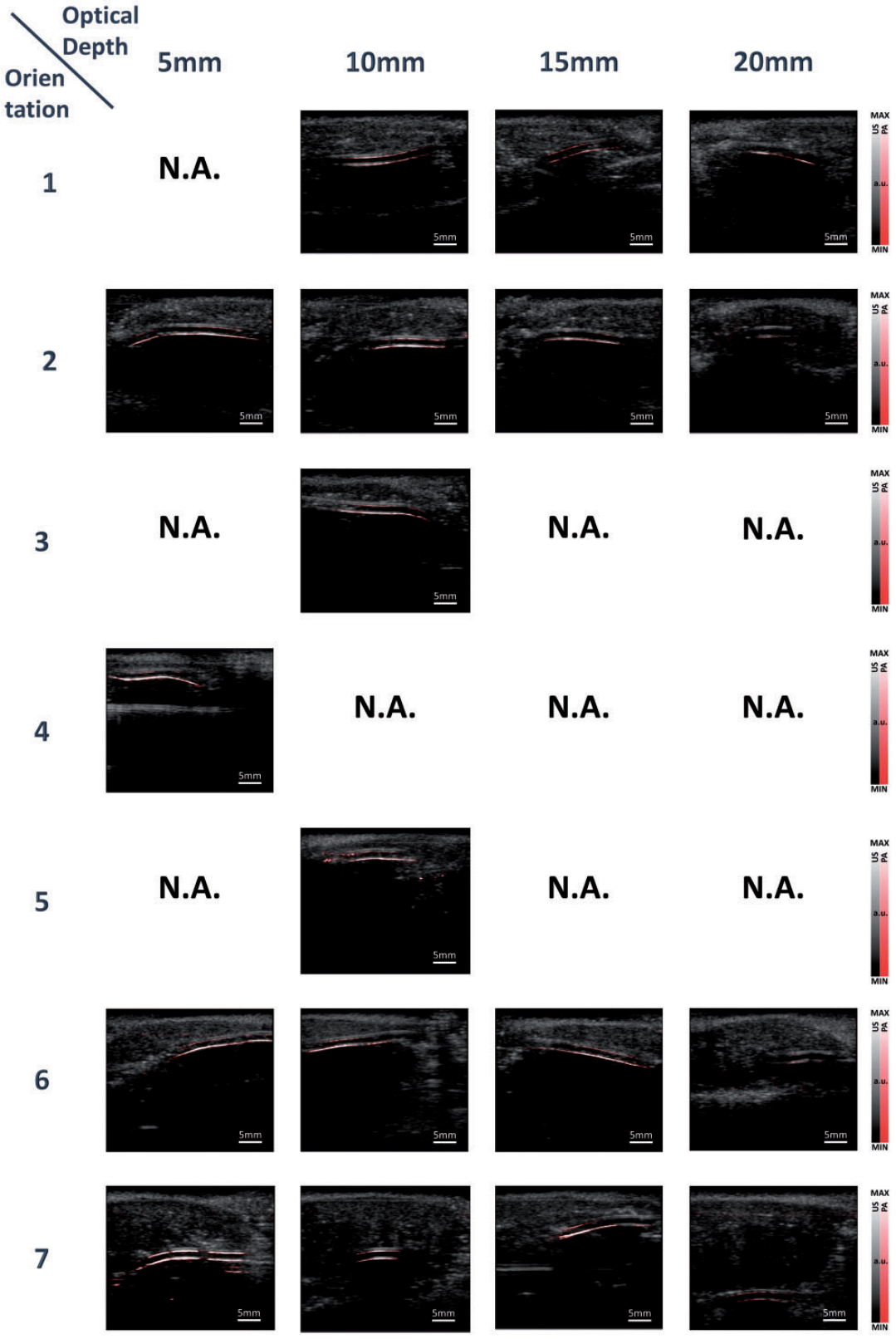

Figure 2. PA and US combined imaging of an ICG-containing tube at different positions in a human prostate. The position is defined by the orientation around the urethra (i.e. the number, corresponding to Figure 1) and the distance from the urethra (i.e. the depth). Each image is a combination of a PA image in pseudo color and an US image in gray scale. N.A. indicates that no image was taken at this position, mainly due to the limited thickness of the prostate tissue. (A color version of this figure is available in the online journal.)

reducing the required optical penetration depth, holds potential to benefit a number of clinical applications, such as structural and functional imaging of cardiovascular system or gastrointestinal system.

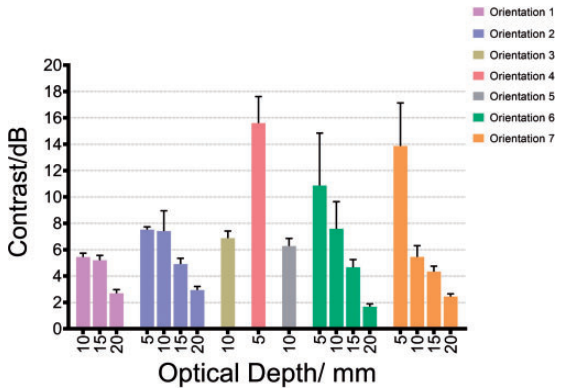

Figure 3. The quantified contrast of PA imaging of the ICG-containing tube over the background prostate tissue quantified at each position in the human prostate. (A color version of this figure is available in the online journal.)

The present study has some limitations. First, due to the safety concern, only limited light fluence can be introduced without damaging the urethral wall. Using the current setting, the optical depth is limited to a 2 cm range around urethra which is not sufficient to cover the entire volume of an extremely large-size prostate. This problem can be solved in the future by further enhancing the detection sensitivity of the PA-US imaging system. In addition, the transurethral light illumination can also be combined with additional transrectal light illumination. With the light introduced from both the urethra and the rectum, the total light energy delivered into a prostate without causing damage can be elevated, and PA imaging can cover a larger volume. Second, in our current feasibility study, the LED array employed was not specially designed for this application. Although the illumination surface the LED array was narrow (6.88 mm), the large housing of the serving circuit prevented the insertion of the LED array into the urethral track in a non-invasive way. In the future, a dedicated LED array with a column shape that suits the urethra track should be designed and fabricated before the clinical trial is

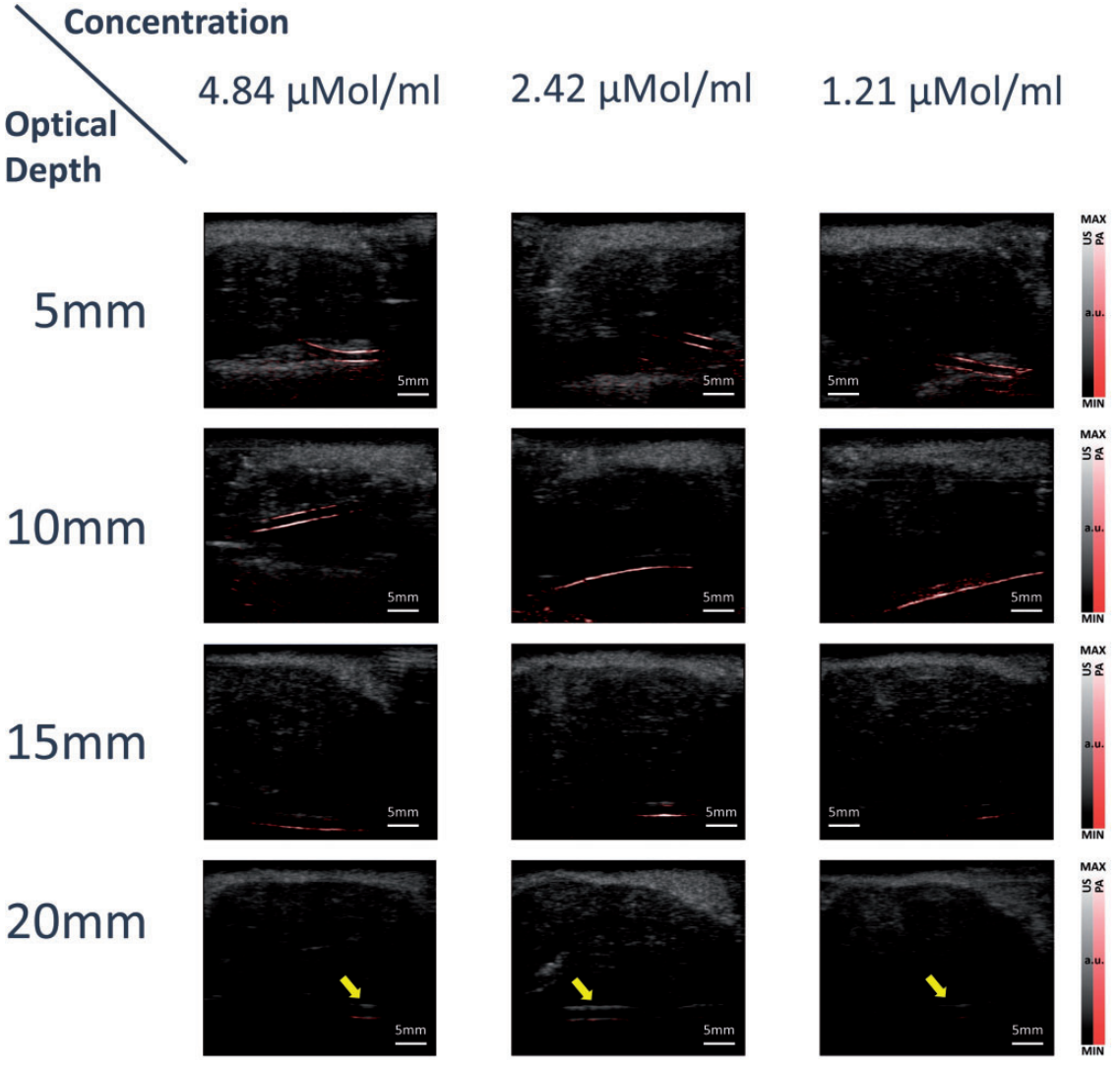

Figure 4. PA and US combined imaging of a tube containing different concentrations of ICG and embedded in a human prostate at different optical depths. (A color version of this figure is available in the online journal.)

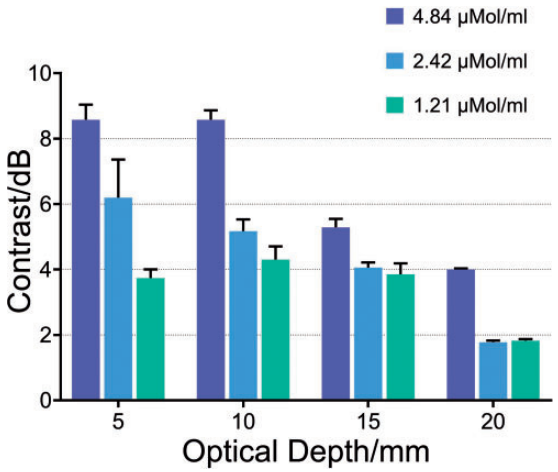

Figure 5. The quantified PA contrast of the ICG-containing tube over the background prostate tissue as a function of the optical depth and the ICG concentration. (A color version of this figure is available in the online journal.)

possible. The large housing of the current LED array is also due to a large cooling board attached to the LEDs. In future design of the LED array, the cooling should also be considered in order to avoid potential thermal damage of the urethral track. Third, in this study on *ex vivo* human tissue samples, we tried to image the samples with the similar anatomical and physiological environments as those *in vivo*. Considering this, whole prostates harvested from radical prostatectomy were employed, and were imaged quickly after the surgeries to keep the samples fresh. By doing so, we expect that both the anatomy and the tissue optical properties in the prostate were similar to those *in vivo*. One limitation of this model is the loss of blood during the surgery which, however, is hard to be avoided for *ex vivo* studies. The reduced blood content could change the light attenuation in the tissue, and affect the accuracy in measuring the imaging depth. Despite these limitations, the knowledges gained from this study focusing on the technical feasibility are valuable, and will contribute to future design for a dedicated imaging system including a miniaturized LED array for studies on human subjects. By then, the clinical feasibility of the proposed imaging technique for prostate cancer detection can be evaluated more comprehensively in a clinical-procedure-equivalent manner.

In conclusion, the technical feasibility of whole prostate molecular imaging realized by transrectal PA imaging with transurethral light illumination was tested on *ex vivo* human prostates. With the optical depth up to 2 cm achieved, PA molecular imaging over the entire volume of a whole human prostate with a regular size is promising. For prostates with larger sizes, 2 cm optical depth can cover at least the transition zones.

Authors' contribution: HZ and SH contributed equally to this paper. Conceptualization, XW and QC; funding acquisition, QC, DW and SH; experiment, HZ, YC, WX, MZ, JP, SH and NS; writing – original draft, HZ; writing – review and editing, XW, QC and SH.

DECLARATION OF CONFLICTING INTERESTS

The author(s) declared no potential conflicts of interest with respect to the research, authorship, and/or publication of this article.

FUNDING

This research was supported by the National Key Research and Development Program of China under grant number 2017YFC0111400, National Natural Science Foundation of China under grant numbers 11674249, 11574231, 81702962, Shanghai Health and family planning commission founding (grant no. 201640051) and Science Lead Supporting project of Shanghai, China 18411961100.

ORCID iD

Haonan Zhang https://orcid.org/0000-0003-0492-6508

REFERENCES

1. van der Poel HG, Buckle T, Brouwer OR, Valdés Olmos RA, van Leeuwen F. Intraoperative laparoscopic fluorescence guidance to the sentinel lymph node in prostate cancer patients: clinical proof of concept of an integrated functional imaging approach using a multimodal tracer. *Eur Urol* 2011;**60**:826–33
2. van den Berg NS, van Leeuwen FWB, van der Poel HG. Fluorescence guidance in urologic surgery. *Curr Opin Urol* 2012;**22**:109–20
3. Yang X, Xiang L. Photoacoustic imaging of prostate cancer. *J Innov Opt Health Sci* 2017;**10**:1730008
4. Yaseen MA. Optoacoustic imaging of the prostate: development toward image-guided biopsy. *J Biomed Opt* 2010;**15**:021310
5. Wang X, Roberts WW, Carson PL, Wood DP, Fowlkes JB. Photoacoustic tomography: a potential new tool for prostate cancer. *Biomed Opt Express* 2010;**1**:1117
6. Dogra V, Evans K, Ghazi A, Joseph J, Messing E, Rao N, Valluru K, Yao J, Chinni B. Multispectral photoacoustic imaging of prostate cancer: preliminary ex-vivo results. *J Clin Imaging Sci* 2013;**3**:41
7. Horiguchi A, Shinchi M, Nakamura A, Wada T, Ito K, Asano T, Shinmoto H, Tsuda H, Ishihara M. Pilot study of prostate cancer angiogenesis imaging using a photoacoustic imaging system. *Urology* 2017;**108**:212–9
8. El-Gohary SH, Metwally MK, Eom S, Jeon SH, Byun KM, Kim T-S. Design study on photoacoustic probe to detect prostate cancer using 3D monte carlo simulation and finite element method. *Biomed Eng Lett* 2014;**4**:250–7
9. Tang S, Chen J, Samant P, Stratton K, Xiang L. Transurethral photoacoustic endoscopy for prostate cancer: a simulation study. *IEEE Trans Med Imaging* 2016;**35**:1780–7
10. Lediju Bell MA, Guo X, Song DY, Boctor EM. Transurethral light delivery for prostate photoacoustic imaging. *J Biomed Opt* 2015;**20**:036002
11. Agarwal A, Huang SW, O'Donnell M, Day KC, Day M, Kotov N, Ashkenazi S. Targeted gold nanorod contrast agent for prostate cancer detection by photoacoustic imaging. *J Appl Phys* 2007;**102**:064701
12. Kothapalli S, Ma T-J, Vaithilingam S, Oralkan O, Khuri-Yakub BT, Gambhir SS. Deep tissue photoacoustic imaging using a miniaturized 2-D capacitive micromachined ultrasonic transducer array. *IEEE Trans Biomed Eng* 2012;**59**:1199–204
13. Levi J, Sathirachinda A, Gambhir SS. A high-affinity, high-stability photoacoustic agent for imaging gastrin-releasing peptide receptor in prostate cancer. *Clin Cancer Res* 2014;**20**:3721–9
14. Xu G, Qin M, Mukundan A, Siddiqui J, Takada M, Vilar-Saavedra P, Tomlins SA, Kopelman R, Wang X. Prostate cancer characterization by

optical contrast enhanced photoacoustics. In Oraevsky AA, Wang LV (eds) *Proc SPIE Photons Plus Ultrasound:Imaging and Sensing 2016*, San Francisco, CA, USA, 2016, pp. 97080I–97086
15. Zhang HK, Chen Y, Kang J, Lisok A, Minn I, Pomper MG, Boctor EM. Prostate-specific membrane antigen-targeted photoacoustic imaging of prostate cancer *in vivo*. *J Biophotonics* 2018;**11**:e201800021
16. Zhu Y, Xu G, Yuan J, Jo J, Gandikota G, Demirci H, Agano T, Sato N, Shigeta Y, Wang X. Light emitting diodes based photoacoustic imaging and potential clinical applications. *Sci Rep* 2018;**8**:9885
17. Commission, I. E. IEC 62471:2006 (2006) Photobiological safety of lamps and lamp systems. International Standard, http://tbt.testrust.com/image/zt/123/100123_2.pdf (accessed 26 November 2018)

(Received August 7, 2019, Accepted September 27, 2019)